JOURNAL OF PLANKTON RESEARCH | VOLUME 23 | NUMBER 10 | PAGES 1137–1145 | 2001

Multiscale patchiness of the calanoid copepod *Temora longicornis* in a turbulent coastal sea

LAURENT SEURONT[1,3] AND YVAN LAGADEUC[2]

[1]OCEAN ECOSYSTEM DYNAMICS LABORATORY, DEPARTMENT OF OCEAN SCIENCE, TOKYO UNIVERSITY OF FISHERIES, 4-5-7 KONAN, MINATO-KU, TOKYO 108, JAPAN. [2]LABORATOIRE DE BIOLOGIE ET BIOTECHNOLOGIES MARINE, IUT GÉNIE BIOLOGIQUE, UNIVERSITÉ DE CAEN, BD DU MARÉCHAL JUIN, F-14032 CAEN CEDEX, FRANCE

[3]PRESENT ADDRESS: STATION MARINE DE WIMEREUX, CNRS UPRES-A 8013 ELICO, UNIVERSITÉ DES SCIENCES ET TECHNOLOGIES DE LILLE, BP 80, F-62930 WIMEREUX, FRANCE

We present evidence that intermittent variability in zooplankton abundance can be characterized in terms of multifractals. A 3-min-resolution time series of abundance in the calanoid copepod Temora longicornis, taken from a fixed mooring in the coastal waters of the Eastern English Channel for 66 h, provided the data for our analysis. The multifractal nature of the distribution of T. longicornis abundance appears to be very different from those of purely passive scalars (i.e. temperature and salinity), and also from phytoplankton biomass over a similar range of scales in similar environments. Finally, we show that the multifractal distribution of T. longicornis can be wholly described by three basic parameters in the framework of universal multifractals, opening up very large perspectives for

INTRODUCTION

Heterogeneity in the distribution of zooplankton has been recognized for many years [e.g. (Hardy, 1936)] and has since received a considerable amount of attention (Mackas *et al.*, 1985; Davis *et al.*, 1991). However, the phenomenon has seldom been described precisely, although zooplankton patchiness is relevant to many aspects of biological oceanography (Daly and Smith, 1993). Quantitative analyses of zooplankton spatial patterns in the ocean using time series analysis and power spectral analysis (Mackas and Boyd, 1979; Tsuda *et al.*, 1993), and more recently fractal analysis (Tsuda, 1995), have generated a large body of observational and theoretical work [e.g. (Powell and Okubo, 1994)], motivating a new field of marine research devoted to the characterization of intermittent patterns in the framework of multifractals (Pascual *et al.*, 1995; Seuront *et al.*, 1996a,b, 1999).

Multifractals can be viewed as a generalization of fractal geometry (Mandelbrot, 1983) initially introduced to describe the relationship between a given quantity and the scale at which it is measured. While fractal geometry describes the structure of a given pattern with the help of only one parameter (i.e. the so-called fractal dimension), multifractals characterize its detailed variability by an infinite number of sets, each with its own fractal dimension. More precisely, multifractal approaches, which do not require any statistical preconception of the data, provide very good approximations—at all scales and all intensities—of the statistics of intermittently fluctuating patterns, and determine the probability distribution of the pattern values [see Pascual *et al.* (Pascual *et al.*, 1995) and Seuront *et al.* (Seuront *et al.*, 1999) for further details]. Moreover, one statistical consequence of intermittency is a strong departure from Gaussianity (Baker and Gibson, 1987). Multifractals provide a more suitable alternative to the basic random walk and spectral methods implicitly based on Gaussian, or quasi-Gaussian, statistics [see e.g. (Peitgen *et al.*, 1992)]. Thus, considering that in the general background of spatio-temporal intermittency encountered in the ocean [e.g. (Platt *et al.*, 1989)], knowledge of the underlying statistics of any intermittent fields may avoid the bias introduced by chronic undersampling of an intermittent signal (Bohle-Carbonel, 1992), a stochastic multifractal framework is particularly well suited to describe the structure of quantities that vary intermittently in space and time, such as phytoplankton and zooplankton distributions (Pascual *et al.*, 1995; Seuront *et al.*, 1996a,b, 1999).

Knowledge of the distribution of particles is essential in understanding the trophic transaction mechanisms that

regulate the flows of energy and matter in the ocean (Davis *et al.*, 1991). Indeed, both phytoplankton and zooplankton biomass are concentrated in numerous zones of continuously varying sizes and concentrations, and the food signal generated by such complex structures has characteristics that traditional approaches using statistics based on spatial or temporal homogeneity are unable to resolve (Rothschild, 1992). Moreover, previous observations conducted on zooplankton distributions indicate that, generally, larger life forms show more extreme spatial scale aggregations than do smaller and less mobile organisms (Mackas and Boyd, 1979; Mackas *et al.*, 1985; Daly and Smith, 1993). An understanding of pelagic ecosystem structure and function then requires precise estimates of both predator and prey abundances, i.e. spatial patterns of phytoplankton and zooplankton.

In particular, the calanoid copepod *Temora longicornis*, which is very abundant in coastal temperate waters of the northern hemisphere, appears to be of great ecological significance. Indeed, *T. longicornis* represents 35–70% of the total population of copepods in the Southern Bight of the North Sea (Daan, 1989), and in Long Island Sound (USA) is able to remove up to 49% of the daily primary production (Dam and Peterson, 1993). Motivated by the ecological significance of this organism, and following the recent empirical investigations conducted on phytoplankton distributions in the highly dissipative waters of the Eastern English Channel and the Southern Bight of the North Sea (Seuront *et al.*, 1996a,b, 1999), the aim of this paper is to investigate the distribution of the calanoid copepod *T. longicornis* in order to provide further insights into the trophic interactions occurring in such turbulent coastal ecosystems.

METHOD

Study area and sampling

Sampling was conducted from 1 to 3 April 1997 in the Eastern English Channel for 66 h (~5.5 tidal cycles). The tidal range in this system is one of the largest in the world (ranging from 3 to 9 m). Tides present a residual circulation parallel to the coast, with nearshore coastal waters drifting from the English Channel into the North Sea. Coastal waters are influenced by freshwater run-off from the Seine estuary to the Straits of Dover, and separated from offshore waters by a tidally maintained frontal area [(Brylinski and Lagadeuc, 1990; Lagadeuc *et al.*, 1997); Figure 1). The sampling location was chosen because its physical and hydrological properties are representative of the coastal water flow encountered in the Eastern English Channel (Lizon *et al.*, 1995; Lizon and Lagadeuc, 1998) where *T. longicornis* is known to be very abundant and dominates the zooplankton (Brylinski and Lagadeuc, 1988).

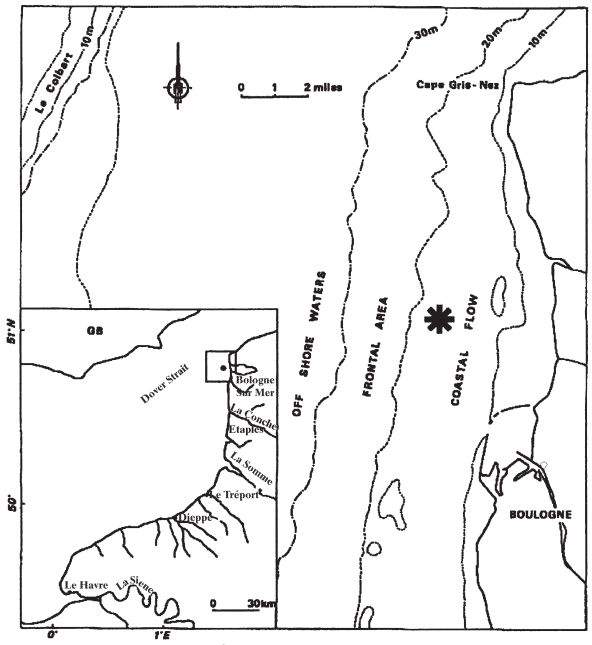

Fig. 1. Study area and location of the sampling station (*) along the French coast of the Eastern English Channel.

Since our aim was to investigate the horizontal distribution of *T. longicornis*, water was continuously taken from a depth of 10 m through a weighted sea water intake, and directly brought through a 200-μm-mesh plankton net by means of a Flight pump with an output of 300 l min^{-1}, connected to 10-cm-diameter plastic tubing. Every 3 min, filtered organisms were collected and immediately preserved in a 10% formaldehyde solution. The adult males and females from the 1321 collected samples were subsequently counted under a dissecting microscope. Figure 2 shows the resulting time series of the abundance of the

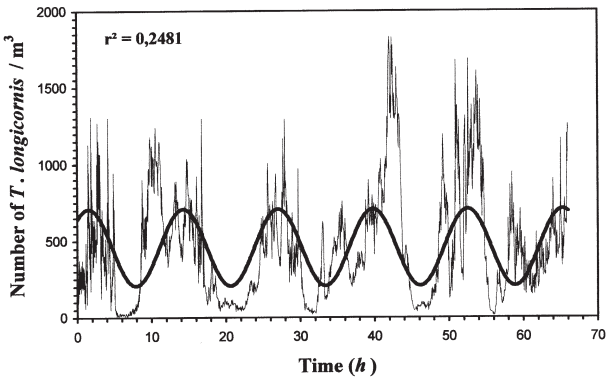

Fig. 2. Time series of *T. longicornis* abundance (ind. m^{-3}) recorded at 10 m depth in the Eastern English Channel, shown together with the best tidal sinusoidal fit.

adult *T. longicornis*, which shows significant 12.5 h cycle, but exhibits a very intermittent 'background'.

Data analysis

After detrending, the scaling properties of empirical fields are usually tested using Fourier power spectrum analysis, leading to a characteristic power-law form:

$$E(f) \approx f^{\beta} \tag{1}$$

where f is frequency. This form indicates the absence of characteristic time scale in the range of the power law, i.e. a scaling behavior. The power-law form will appear approximately linear when plotted on a log–log scale. The exponent β and the fractal dimension D are related according to (Feder, 1988):

$$D_d = d - (3 - \beta)/2 \tag{2}$$

where d is the Euclidean dimension of the observation space (i.e. $d = 1$ for time series). From equation (2), it can be seen that comparisons between the fractal dimensions derived from one-dimensional and d-dimensional datasets require a standardization procedure. All the fractal dimensions D referred to and discussed hereafter have thus simply been standardized from the d-dimensional fractal dimensions, D_d, into a one-dimensional reference framework by taking the difference $D = D_d - (d - 1)$ (Schroeder, 1991).

However, power spectral analysis, implicitly assuming 'quasi-Gaussian' statistics and limited to a second-order statistic (i.e. the variance), very poorly characterizes quantities that vary intermittently (i.e. occasional and unpredictable large peaks separated by very low values). We then adopt an empirical generalization of the widely used power spectral approach with the help of the qth-order structure functions (Monin and Yaglom, 1975; Anselmet *et al.*, 1984):

$$\langle(\Delta Zoo_{\tau})^{q}\rangle \approx \tau^{\zeta(q)} \tag{3}$$

where ΔZoo_{τ} is the fluctuation of the abundance of *T. longicornis* at scale τ and angle brackets '<.>' indicate an average which is performed for all points of the *T. longicornis* abundance time series separated by a distance τ [i.e. $\langle(\Delta Zoo_{\tau})^{q}\rangle$ are the statistical moments of the fluctuation]. The scaling exponent $\zeta(q)$ is estimated by the slope of the linear trends of $\langle(\Delta Zoo_{\tau})^{q}\rangle$ versus τ in a log–log plot. Equation (3) gives the scale-invariant structure functions exponent E(q), which characterizes the statistics of the whole field. In particular, the first moment gives the scaling exponent $H = \zeta(1)$, corresponding to the scale dependency of the average fluctuations: if $H \neq 0$, the fluctuations (ΔZoo_{τ}) will depend on the time scale; it therefore characterizes the degree of stationarity of the process. The second moment is linked to the slope, β, of the power spectrum by $\beta = 1 + \zeta(2)$. For simple scaling (fractal) processes, the scaling exponent of the structure function $\zeta(q)$ is linear [$\zeta(q) = q/2$ for Brownian motion and $\zeta(q) = q/3$ for non-intermittent turbulence]. For multifractal processes, this function is non-linear and convex (Seuront *et al.*, 1999).

A priori, the function $\zeta(q)$ could depend on a very large number—even an infinity—of parameters; therefore, a very large number of its estimates for different values of q would be necessary. However, in the frame of universal multifractals (Schertzer and Lovejoy, 1987, 1989), $\zeta(q)$ is determined by only three parameters:

$$\zeta(q) = qH - \frac{C_1}{(\alpha - 1)}(q^{\alpha} - q) \tag{4}$$

where H is still given by $H = \zeta(1)$; the second term [i.e. the scaling moment function $K(q)$] characterizes the statistical behavior of a given intermittent process; [see (Seuront *et al.*, 1999)].

$$K(q) = \frac{C_1}{(\alpha - 1)}(q^{\alpha} - q) \tag{5}$$

expresses the departure from homogeneity [in which case $\zeta(q) = qH$] due to intermittency of the process. C_1 is a co-dimension that characterizes the sparseness of the process, and is bounded between $C_1 = 0$ for a homogeneous space-filling process and $C_1 = d$, where d is the dimension of the space supporting the considered process, with $d = 1$ for time series. With a low C_1 value (i.e. close to 0), the field is close to its mean value almost everywhere; a large C_1 is characteristic of a field that has very low values almost everywhere, except in some rare and sparse locations where it takes values much greater than its mean value. The Lévy index α varies between a minimum of 0 (corresponding to a monofractal pattern) and a maximum of 2 (corresponding to a log–normal multifractal case), and indicates the degree of multifractality. As α increases, the more numerous are the variability levels bounded between lower and higher values of the process.

There are several ways to estimate the universal multifractal indices C_1 and α [see (Seuront *et al.*, 1996a,b, 1999)]. However, we can easily estimate C_1 and α from equation (4): if equation (4) is differentiated and evaluated at $q = 0$, simple algebra shows that:

$$q\zeta'(0) - \zeta(q) = \frac{C_1 q^{\alpha}}{(\alpha - 1)} \tag{6}$$

Thus, a log–log plot of $[q\zeta'(0) - \zeta(q)]$ versus q will yield a straight line. The slope of the line is given by α and the corresponding C_1 value can be estimated by the intercept

(Schmitt *et al.*, 1995). Once we know the parameter values, we can completely characterize the underlying multifractal process in a spatial or temporal variation. Finally, for a detailed discussion of what can be concluded ecologically from the use of multifractal algorithms, one may refer to Pascual *et al.* (Pascual *et al.*, 1995) and Seuront *et al.* (Seuront *et al.*, 1999).

RESULTS

The log–log plot of the zooplankton power spectrum shows a single scaling regime from smaller to larger scales, i.e. $E(f) \approx f^{\beta}$ with $\beta = 1.42$ (Figure 3). This indicates that the same process, or at least similar processes, can be regarded as being responsible for the scaling structure of the abundance of *T. longicornis* from time scales ranging from 6 min to 66 h. This range of temporal scales can be converted into spatial scales using 'Taylor's hypothesis of frozen turbulence' (Taylor, 1938), which basically states that temporal and spatial averages t and l, respectively, can be related by a constant velocity v: $l = v \cdot t$. Then, using the mean instantaneous tidal circulation of 0.509 m s^{-1} observed during the field experiment at the sampling depth, the associated spatial scales range between 92 m and 120 km. Finally, the power spectral exponent β estimated over this range of scales can be converted to a fractal dimension following equation (2) as $D = 1.79$.

This result can be confirmed and generalized by the qth-order structure functions (Figure 4). Thus, it clearly appears that for values of q ranging from 1 to 3, $<(\Delta Z_{00_\tau})^q>$ exhibits linear trends over the whole range of available time scales. The different values of the empirical exponent $\zeta(q)$ were calculated for a range of q values from 0 to 3 in increments of 0.1. The empirical curve is clearly non-linear, even for moments $q < 1$, showing that the abundance fluctuations of *T. longicornis* can be regarded as multifractal over the time scales ranging from 6 min to 66 h (Figure 5). In particular, the scaling of the first moment gives $H = \zeta(1) = 0.58$, indicating that the temporal distribution of *T. longicornis* is far from conservative, or stationary (in which case $H = 0$). The scaling of the second-order moment confirms the estimate from the power spectrum: (2) = 0.41 [i.e. $\beta = 1 + \zeta(2)$].

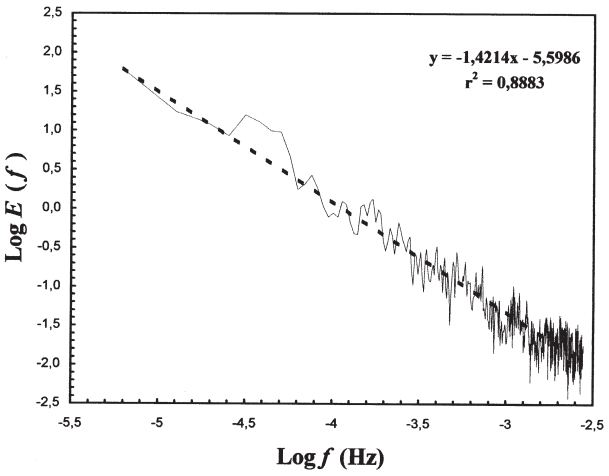

Fig. 3. The power spectrum of the *T. longicornis* abundance data, shown in a log–log plot. The overall straight line $f^{-1.42}$ is an indication of scaling for frequencies ranging from 6 min to 66 h^{-1}.

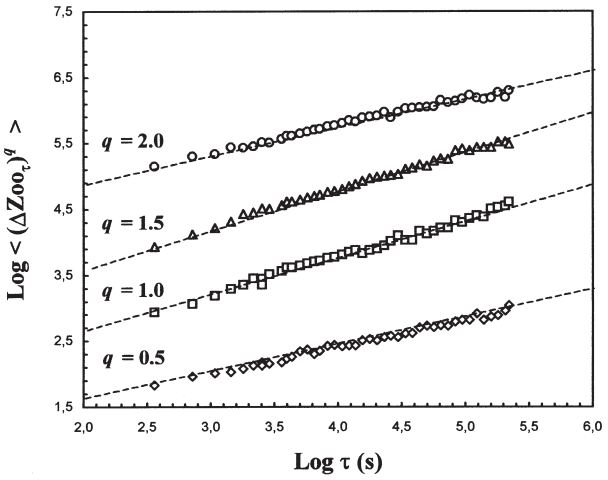

Fig. 4. The structure functions $<(\Delta Z_{00_\tau})^q>$ versus τ in a log–log plot for q = 0.5, 1, 1.5 and 2. Linear trends are clearly visible for all orders of moments, for a range of scales ranging from 6 min to 66 h. The straight lines indicate the best linear regression over this range of scales for each value of q. This gives in particular $H = \zeta(1) = 0.58$, and $\zeta(2) = 0.41$.

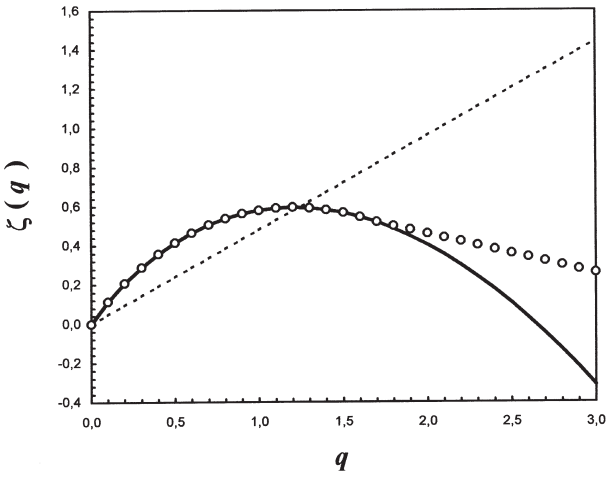

Fig. 5. The scaling exponent structure function $\zeta(q)$ empirical curve (circles) compared to the monofractal curve $\zeta(q) = qH$ (dashed line), and to the universal multifractal function (thick continuous line) obtained with $\alpha = 1.6$ and $C_1 = 0.44$ in equation (4). The universal multifractal fit is excellent until moment order $q_{max} = 1.7$, corresponding to a multifractal phase transition occurring because of sampling limitations.

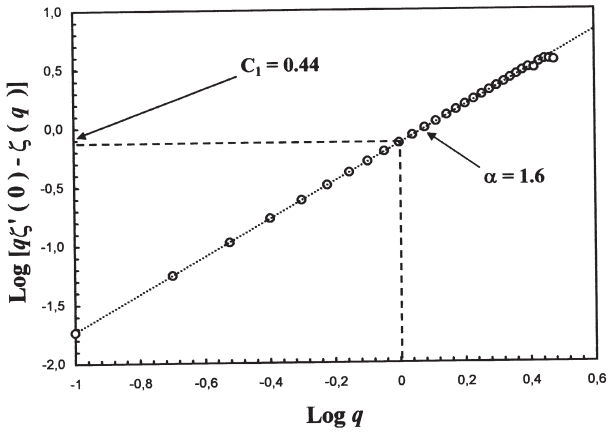

Fig. 6. Empirical curve $[q\zeta'(0) - \zeta(q)]$ versus q in a log–log plot providing direct estimates of the universal multifractal parameters C_1 and α. α is the slope of the straight line and C_1 is estimated by the intercept; therefore, $\alpha = 1.6$ and $C_1 = 0.44$.

We now estimate the universal parameters α and C_1 from equation (6). Figure 6 shows that $\alpha = 1.6 \pm 0.1$ and $C_1 = 0.44 \pm 0.02$, the error bars come from comparison between these α and C_1 estimates and those obtained using the technique (Lavallée, 1991; Lavallée *et al.*, 1992), which we also applied to the data and which have been extensively described elsewhere [see (Seuront *et al.*, 1999)]. The theoretical curve corresponding to these values substituted into equation (4) is shown in Figure 5 by a thick continuous line. The universal multifractal fit is excellent until moment order $q_{max} = 1.7$, after which the empirical curve (dots) is linear. This linear behavior of the empirical scaling exponent structure function $\zeta(q)$ for sufficiently high order moments is well known (Schertzer and Lovejoy, 1989) and is due to sampling limitations (Seuront *et al.*, 1999).

DISCUSSION

The recognition of patchiness is hardly new to plankton ecology; it was described in zooplankton communities over a century ago (Haeckel,1891). However, if a distribution is patchy, then conventional statistical methods become less useful as analytical tools due to violations in basic assumptions such as randomness. Thus, the main advantage of our multifractal approach is that it does not require any preconceptions of the data. In an intermittent setting, it should then be regarded as an alternative to the widely used spectral methods, implicitly based on Gaussian statistics [e.g. (Platt and Denman, 1975)], as well as the more recently developed one-dimensional neighbor techniques devoted to estimating zooplankton patch size and based on an untenable assumption of a regular distribution of patches (Shiyomi and Yamamura, 1993; Currie *et al.*, 1998). In particular, both the fractal and universal multifractal frameworks used here characterize the structure of the overall variability of a given intermittent pattern with, respectively, one and three basic parameters, and then allow direct comparisons to be made between biological and physical fields.

Our fractal dimension estimates of the *T. longicornis* distribution can then be compared with those estimated from oceanic turbulence and both phytoplankton and zooplankton distributions. Reported fractal dimensions of two-dimensional oceanic turbulence range from 1.2 to 1.4 (Osborne *et al.*, 1989; Osborne and Caponio, 1990; Sanderson and Booth, 1991), while the theoretical spectral exponent $\beta = 3$ (Kraichnan, 1967) of two-dimensional turbulence leads to a fractal dimension $D = 1$. On the other hand, in three-dimensional turbulence, the fractal dimension related to the theoretical spectral exponent $\beta = 5/3$ expected in the case of a purely passive scalar (Kolmogorov, 1941) is $D = 1.67$. Therefore, the estimated fractal dimensions for *T. longicornis* distribution ($D = 1.79$) are significantly higher than those of oceanic turbulence. This fractal dimension is also higher than those of phytoplankton distributions estimated from *in vivo* fluorescence time series in the Southern Bight of the North Sea and the Eastern English Channel [$D \in [1.61–1.67]$; (Seuront *et al.*, 1996a,b, 1999)] as from satellite images of sea surface chlorophyll patterns [i.e. $D \in [0.98–1.69]$; e.g. (Denman and Abbott, 1988, 1994; Smith *et al.*, 1988)]. The fact that phytoplankton and zooplankton differ in terms of size and motility suggests that copepod behaviors such as diel migration, phototaxis, rheotaxis, social behaviors and predation pressure—behaviors relevant at the space and time scales of the present study—induce larger fractal dimensions (i.e. flatter power spectrum and weaker scale dependence) in comparison with phytoplankton. Numerical experiments based on simple predator–prey formulations considered in a turbulent frame seem to support this hypothesis. Steele and Henderson (Steele and Henderson, 1992) then demonstrated that the interactions between diel vertical migration and turbulent shear could lead to a flatter zooplankton power spectrum, while Powell and Okubo (Powell and Okubo, 1994) reached similar conclusions from their study of interacting plankton populations in two-dimensional turbulence. Finally, one may note that the fractal distribution estimated here from the distribution of *T. longicornis* is very similar to that estimated for the oceanic copepod *Neocalanus cristatus* abundance transects from the subarctic Pacific, i.e. $D = 1.80$ (Tsuda, 1995), over a similar range of scales (i.e. between tens of meters and >100 km), suggesting that the distribution of zooplankton species could be very similar independent of their surrounding environments.

Comparisons of the universal multifractal parameters estimated in the present study with those of other phytoplankton and zooplankton datasets has led to further results. The values of the parameter H ($H = 0.58$) and C_1 (C_1) estimated in the present study are then obviously higher than those of phytoplankton biomass over similar ranges of scales, i.e. $H \in [0.12–0.34]$ and $C_1 \in [(0.02–0.05]$ (Seuront *et al.*, 1996a,b, 1999). This result implies that zooplankton distributions are less conservative and more sparse (i.e. characterized by low values, except in some rare and sparse location where it takes large values much greater than the mean value) than those of phytoplankton. On the contrary, the parameter $\alpha = 1.60$ is within the range of α values estimated for phytoplankton distributions (Seuront *et al.*, 1996a, b, 1999). These high α values indicate that intermittencies of all magnitudes contribute significantly to the multifractal processes underlying our measured *T. longicornis* abundance. In other words, we are very far from the monofractal case. The differences found between the values of the parameters H and C_1 for zooplankton and phytoplankton then confirm the observations conducted in the monofractal frame concerning the influence of zooplankton mobility on their spatial distribution. These differences also confirm that, generally, larger life forms show more extreme spatial scale aggregations than do smaller and less mobile organisms, which in the multifractal sense corresponds to larger C_1 values. One may also note that the D_q multifractal formalism used by Pascual *et al.* (Pascual *et al.*, 1995) can be related to our scaling moment function $K(q)$ formalism as:

$$D_q = d - K(q) \tag{7}$$

where d is the Euclidean dimension of the observation space (i.e. $d = 1$ for time series and transects). In particular, we have $D_2 = 1 - K(2)$, leading to $D_2 \approx 0.38$ from Pascual *et al.* (Pascual *et al.*, 1995) and $D_2 \approx 0.24$ from the present study. This suggests a higher intermittency perceptible in our dataset. However, this difference might also be due to the better quality and resolution of the present dataset, as the acoustic data analyzed by Pascual *et al.* (Pascual *et al.*, 1995) were constructed by averaging measurements vertically and hourly, and also corresponded to a multispecies zooplankton assemblage.

Multifractals, and in particular universal multifractals, lead to a very precise characterization of the overall statistical structure of any given intermittent pattern (with the help of the three basic empirical parameters). Thus, they appear to be an efficient descriptive tool which should also allow modeling of the multiscale detailed variability of intermittently fluctuating biological fields as well as one of the properties of their surrounding environment [see (Seuront *et al.*, 1999) for further discussions]. In particular, using the modeling techniques detailed in Pecknold *et al.* (Pecknold *et al.*, 1993), a simulation of the copepod horizontal distribution based on the estimated multifractal parameters $H = 0.58$, $C_1 = 0.44$ and $\alpha = 1.60$ has been performed (Figure 7). Figure 7 shows a two-dimensional simulation of the *T. longicornis* distribution, which clearly exhibits very intermittent behavior associated with the occurrence of a few high-density patches over a wide range of low-density patches. Analysis of these data using multifractal modeling is a potentially powerful alternative to physical models of turbulence, which lead to the parameterization of the effects of turbulence on plankton distribution. Indeed, these models, incorporating diffusive processes [e.g. (Okubo, 1980)], non-diffusive advection (Abraham, 1998), or coupling fluid-dynamic models of quasi-geostrophic turbulence, multi-compartment ecosystem dynamics and seasonal forcing (Smith *et al.*, 1996), can describe certain, but not all, aspects of turbulence and are often far from comprehensive (Visser, 1997). The advantages of universal multifractal simulation techniques are essentially the small number of input parameters (only the three basic parameters H, C_1 and α), the low computation time involved (only a few seconds on a Pentium II for a 512×512 field) and their stochasticity. This framework avoids numerical artifacts linked, for instance, to the sensitivity to initial conditions encountered when using models dealing with the Navier–Stokes equation or with systems of differential equations.

Precise knowledge of the distribution of pelagic organisms is indeed of fundamental importance in understanding the trophic relationships between organisms and also the related fluxes of matter. For instance, the distribution of prey organisms is very important for predators, as recently numerically investigated (Seuront, 2001; Seuront *et al.*, 2001), because food availability changes depending on the dimension. Low fractal dimension means a smooth and predictable distribution of particles gathered in small numbers of patches, and high dimension means rough, fragmented, space-filling and less predictable distribution. Therefore, when a predator can remotely detect its surroundings, prey distributions with low dimension should be more efficient. In contrast, when a predator has no detection ability, prey distributions with high dimension should be relatively better, because available food quantity or encounter rate becomes proportional to the searched volume as fractal dimension increases. Moreover, the very complex patchy structure associated with a multifractal distribution may also change the nature of the food signal, usually regarded as homogeneously distributed in space and time in models of predator–prey encounter rates [see Dower *et al.* (Dower *et al.*, 1997) for a review]. Indeed, planktonic animals have been shown to remain within

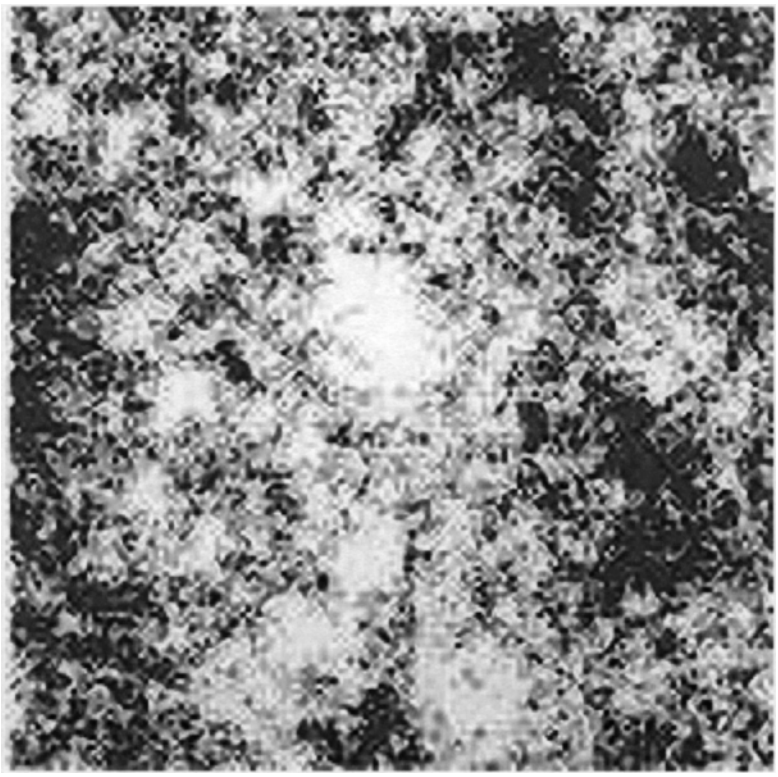

Fig. 7. A two-dimensional simulation of *T. longicornis* using the empirical estimates of the universal multifractal parameters $H = 0.58$, $C_1 = 0.44$ and $\alpha = 1.6$. Black and white values are high and low zooplankton concentrations, respectively.

patches when feeding (Price, 1989), or exhibit more fine-scale movements in areas of higher food concentration (Bundy *et al.*, 1993). Thus, encounter rates might be very different when organisms feed within patches (intensive search) as opposed to the search for new patches (extensive search), as has been described in the foraging behavior of beetles (Ferran and Dixon, 1993). Thus, foraging models will probably incorporate switching between feeding and searching behaviors as scaled to organism size, in order to simulate these complex physical–biological relationships effectively (Noda *et al.*, 1992).

Plankton patchiness has now been widely recognized as a difficult problem in marine ecosystem studies, because of both conceptual and technical limitations [e.g. (Platt *et al.*, 1989)]. The descriptive analysis and modeling tools shown in the present study demonstrate that only three parameters are needed to accurately describe and reconstruct the patchy structure of the horizontal distribution of the pelagic copepod *T. longicornis*. Thus, as propounded in recent studies in different fields of the geophysical sciences (Schmitt *et al.*, 1995, 1998; Liu and Molz, 1997; Schertzer *et al.*, 1997), we believe that multifractals could become an extremely efficient tool to introduce heterogeneous distributions of organisms into ecological models.

ACKNOWLEDGEMENTS

We thank J. Harlay, A. Lefebvre and D. Saïu for their help during the sea experiment, and F. Berreville, O. Borot, S. Coulomb, J. Harlay, D. Hilde and S. Jaskulski for their help in copepod counting. Thanks are extended to the captain and the crew of the NO 'Côte de la Manche' for their assistance during the cruise. We are grateful to Ms V. Pasour who kindly edited the English language, and to one anonymous referee who greatly improved the quality of a previous version of this work.

REFERENCES

Abraham, E. R. (1998) The generation of plankton patchiness by turbulent stirring. *Nature*, **391**, 577–580.

Anselmet, F., Gagne, Y., Hopfinger, E. J. and Antonia, R. A. (1984) High-order velocity structure functions in turbulent shear flows. *J. Fluid Mech.*, **140**, 63–69.

Baker, M. A. and Gibson, C. H. (1987) Sampling turbulence in the stratified ocean: statistical consequences of strong intermittency. *J. Phys. Oceanogr.*, **17**, 1817–1836.

Bohle-Carbonel, M. (1992) Pitfalls in sampling, comments on reliability and suggestions for simulation. *Cont. Shelf Res.*, **12**, 3–14.

Brylinski, J. M. and Lagadeuc, Y. (1988) Influence du coefficient de la

marée sur la répartition côte-large d'une espèce planctonique à affinités côtières: *Temora longicornis* (Crustacé, Copépode). *C. R. Acad. Sci. Paris Sér. II*, **307**, 183–187.

Brylinski, J. M. and Lagadeuc, Y. (1990) L'interface eau côtière/eau du large dans le Pas-de-Calais (côte française): une zone frontale. *C. R. Acad. Sci. Paris Sér. 2*, **311**, 535–540.

Bundy, M. H., Gross, T. F., Coughlin, D. J. and Strickler, J. R. (1993) Quantifying copepod searching efficiency using swimming pattern and perceptive ability. *Bull. Mar. Sci.*, **53**, 15–28.

Currie, W. J. S., Claereboudt, M. and Roff, J. C. (1998) Gaps and patches in the ocean: a one-dimensional analysis of planktonic distributions. *Mar. Ecol. Prog. Ser.*, **171**, 15–21.

Daan, R. (1989) Factors controlling the summer development of the copepod populations in the Southern Bight of the North Sea. *Neth. J. Sea Res.*, **23**, 305–322.

Daly, K. L. and Smith, W. O. (1993) Physical–biological interactions influencing marine plankton production. *Annu. Rev. Ecol. Syst.*, **24**, 555–585.

Dam, H. G. and Peterson, W. T. (1993) Seasonal contrasts in the diel vertical distribution, feeding behavior and grazing impact of the copepod *Temora longicornis* in Long Island Sound. *J. Mar. Res.*, **51**, 561–594.

Davis, C. S., Flierl, G. R., Wiebe, P. H. and Franks, P. J. S. (1991) Micropatchiness, turbulence and recruitment in plankton, *J. Mar. Res.*, **49**, 109–151.

Denman, K. L. and Abbott, M. R. (1988) Time evolution of surface chlorophyll patterns from cross-spectrum analysis of satellite color images. *J. Geophys. Res.*, **93**, 6789–6798.

Denman, K. L. and Abbott, M. R. (1994) Time scales of pattern evolution from cross-spectrum analysis of advanced very high resolution radiometer and coastal zone color scanner imagery. *J. Geophys. Res.*, **99**, 7433–7442.

Dower, J. F., Miller, T. J. and Leggett, W. C. (1997) The role of microscale turbulence in the feeding ecology of larval fish. *Adv. Mar. Biol.*, **31**, 169–220.

Feder, J. (1988) *Fractals*. Plenum, New York.

Ferran, A. and Dixon, A. F. G. (1993) Foraging behaviour of ladybird larvae (Coleoptera: Coccinellidae). *Eur. J. Entomol.*, **90**, 383–402.

Haeckel, E. (1891) Plankton studien. *Jena Zt. Naturwiss.*, **25**, 232–336.

Hardy, A. C. (1936) Observation in the uneven distribution of oceanic plankton. *Discovery Rep.*, **11**, 511–538.

Kolmogorov, A. N. (1941) The local structure of turbulence in incompressible viscous fluid for very large Reynolds numbers. *Dokl. Akad. Nauk SSSR*, **30**, 299–303.

Kraichnan, R. H. (1967) Inertial ranges in two-dimensional turbulence. *Phys. Fluids*, **9**, 1937–1943.

Lagadeuc, Y., Brylinski, J. M. and Aelbrecht, D. (1997) Temporal variability of the vertical stratification of a front in a tidal Region of Freshwater Influence (ROFI) system. *J. Mar. Syst.*, **12**, 147–155.

Lavallée, D. (1991) Multifractal techniques: analysis and simulation of turbulent fields. PhD Thesis, McGill University, Montréal, Canada.

Lavallée, D., Lovejoy, S., Schertzer, D. and Schmitt, F. (1992) On the determination of universal multifractal parameters in turbulence. In Moffat, K., Tabor, M. and Zaslavsky, G. (eds), *Topological Aspects of the Dynamics of Fluid and Plasmas*. Kluwer, Boston, pp. 463–478.

Liu, H. H. and Molz, F. J. (1997) Multifractal analyses of hydraulic conductivity distributions. *Water Resour. Res.* **33**, 2483–2488.

Lizon, F. and Lagadeuc, Y. (1998) Comparisons of primary production values estimated from different incubation times in a coastal sea. *J. Plankton Res.*, **20**, 371–381.

Lizon, F., Lagadeuc, Y., Brunet, C., Aelbrecht, D. and Bentley, D. (1995) Primary production and photoadaptation of phytoplankton in relation with tidal mixing in coastal waters. *J. Plankton Res.*, **17**, 1039–1055.

Mackas, D. L. and Boyd, C. M. (1979) Spectral analysis of zooplankton spatial heterogeneity. *Science*, **204**, 62–64.

Mackas, D. L., Denman, K. L. and Abbot, M. R. (1985) Plankton patchiness: biology in the physical vernacular. *Bull. Mar. Sci.*, **37**, 652–674.

Mandelbrot, B. (1983) *The Fractal Geometry of Nature*. Freeman, New York.

Monin, A. S. and Yaglom, A. M. (1975) *Statistical Fluid Mechanics: Mechanics of Turbulence*. MIT Press, London.

Noda, M., Kawabata, K., Gushima, K. and Kakuda, S. (1992) Importance of zooplankton patches in foraging ecology of the planktivorous fish *Chromis chrysurus* (Pomacentridae) at Kuchinoerabu Island, Japan. *Mar. Ecol. Prog. Ser.*, **87**, 251–263.

Okubo, A. (1980) *Diffusion and Ecological Problems: Mathematical Models*. Springer-Verlag, New York.

Osborne, A. R. and Caponio, R. (1990) Fractal trajectories and anomalous diffusion for chaotic pattern motions in 2D turbulence. *Phys. Rev. Lett.*, **64**, 1733–1736.

Osborne, A. R., Kirwan, A. D., Provenzale, A. and Bergamasco, L. (1989) Fractal drifter trajectories in the Kuroshio extension. *Tellus*, **41A**, 416–435.

Pascual, M., Ascioti, F. A. and Caswell, H. (1995) Intermittency in the plankton: a multifractal analysis of zooplankton biomass variability. *J. Plankton Res.*, **17**, 1209–1232.

Pecknold, S., Lovejoy, S., Schertzer, D., Hooge, C. and Malouin, J. F. (1993) The simulation of universal multifractals. In Perdang, J. M. and Lejeune, A. (eds), *Cellular Automata: Prospects in Astrophysical Applications*. World Scientific, Singapore, pp. 228–267.

Peitgen, H. O., Jürgens, H. and Saupe, D. (1992) *Chaos and Fractals. New Frontiers of Science*. Springer-Verlag, New York.

Platt, T. and Denman, K. L. (1975) Spectral analysis in ecology. *Annu. Rev. Ecol. Syst.*, **6**, 189–210.

Platt, T., Harrison, W. G., Lewis, M. R., Li, W. K. W., Sathyendranath, S., Smith, R. E. and Vezina, A. F. (1989) Biological production of the oceans: the case for a consensus. *Mar. Ecol. Prog. Ser.*, **52**, 77–88.

Powell, T. M. and Okubo, A. (1994) Turbulence, diffusion and patchiness in the sea. *Philos. Trans. R. Soc. London Ser. B*, **343**, 11–18.

Price, H. J. (1989) Swimming behavior of krill in response to algal patches: a mesocosm study. *Limnol. Oceanogr.*, **34**, 649–659.

Rothschild, B. J. (1992) Applications of stochastic geometry to problems in plankton ecology. *Philos. Trans. R. Soc. London Ser. B*, **336**, 225–237.

Sanderson, L. F. and Booth, D. A. (1991) The fracatal dimension of drifter trajectories and estimates of horizontal eddy-diffusivity. *Tellus*, **43A**, 334–349.

Schertzer, D. and Lovejoy, S. (1987) Physically based rain and cloud modeling by anisotropic multiplicative turbulent cascades. *J. Geophys. Res.*, **92**, 9693–9714.

Schertzer, D. and Lovejoy, S. (1989) Nonlinear variability in geophysics: multifractal analysis and simulation. In Pietronera, L. (ed.), *Fractals: Physical Origin and Consequences*. Plenum, New York, pp. 49–79.

Schertzer, D., Lovejoy, S., Schmitt, F., Chigirinskaya, Y. and Marsan, D. (1997) Multifractal cascade dynamics and turbulent intermittency. *Fractals*, **5**, 427–471.

Schmitt, F., Lovejoy, S. and Schertzer, D. (1995) Multifractal analysis of the Greenland ice-core project climate data. *Geophys. Res. Lett.*, **22**, 1689–1392.

Schmitt, F., Vannitsem, S. and Barbosa, A. (1998) Modeling of rainfall time series using two-state renewal processes and multifractals. *J. Geophys. Res.*, **103**, 23181–23193.

Schroeder, M. (1991) *Fractals, Chaos, Power Laws*. Freeman, New York.

Seuront, L. (2001) Microscale processes in the ocean: why are they so important for ecosystem functioning? *La Mer*, **39**, 1–8.

Seuront, L., Schmitt, F., Lagadeuc, Y., Schertzer, D., Lovejoy, S. and Frontier, S. (1996a) Multifractal analysis of phytoplankton biomass and temperature in the ocean. *Geophys. Res. Lett.*, **23**, 3591–3594.

Seuront, L., Schmitt, F., Lagadeuc, Y., Schertzer, D. and Lovejoy, S. (1996b) Multifractal intermittency of Eulerian and Lagrangian turbulence of ocean temperature and plankton fields. *Nonlin. Proc. Geophys.*, **3**, 236–246.

Seuront, L., Schmitt, F., Lagadeuc, Y., Schertzer, D. and Lovejoy, S. (1999) Universal multifractal analysis as a tool to characterise multiscale intermittent patterns. Example of phytoplankton distribution in turbulent coastal waters. *J. Plankton Res.*, **21**, 877–922.

Seuront, L., Schmitt, F. and Lagadeuc, Y. (2001) Turbulence intermittency, small-scale phytoplankton patchiness and encounter rates in plankton: where do we go from here? *Deep-Sea Res. I*, **48**, 1199–1215.

Shiyomi, M. and Yamamura, K. (1993) Spatial pattern indices based on distances between individuals on a line-segment with finite length. *Res. Popul. Ecol.*, **34**, 321–330.

Smith, C. L., Richard, K. J. and Fasham, M. J. R. (1996) The impact of mesoscale eddies on plankton dynamics in the upper ocean. *Deep-Sea Res. I*, **43**, 1807–1832.

Smith, R. C., Zhang, X. and Michaelsen, J. (1988) Variability of pigment biomass in the California Current System as determined by satellite imagery. 1. Spatial variability. *J. Geophys. Res.,* **93**, 10863–10882.

Steele, J. H. and Henderson, E. W. (1992) A simple model for plankton patchiness. *J. Plankton Res.*, **14**, 1397–1403.

Taylor, G. I. (1938) The spectrum of turbulence. *Proc. R. Soc. London Ser. A*, **164**, 476–490.

Tsuda, A. (1995) Fractal distribution of the oceanic copepod *Neocalanus cristatus* in the subarctic Pacific. *J. Oceanogr.*, **51**, 261–266.

Tsuda, A., Sugisaki, H., Ishimaru, T., Saino, T. and Sato, T. (1993) White-noise-like distribution of the oceanic copepod *Neocalanus cristatus* in the subarctic North Pacific. *Mar. Ecol. Prog. Ser.*, **97**, 39–46.

Visser, A. W. (1997) Using random walk models to simulate the vertical distribution of particles in a turbulent water column. *Mar. Ecol. Prog. Ser.*, **158**, 275–281.

Received on March 16, 2000; accepted on May 15, 2001